Nima Mirzaei

https://doi.org/10.21278/TOF.454029621
ISSN 1333-1124
eISSN 1849-1391

SOLAR COLLECTOR PERFORMANCE ANALYSIS USING ANOVA METHOD

Summary

In this study, the thermal performance of a newly designed solar air heater was examined using a thoughtfully designed and analysed experimental methodology. In the analysis, three factors (collector type, bed height, and airflow rate) were adjusted and their effects on the performance of the system were evaluated; additionally, mesh layers were used to act as absorber plates. The single and counter flow collectors were also examined using different bed heights (3 cm, 5 cm, and 7 cm) at various airflow rates (0.011 kg/s, 0.035 kg/s, and 0.043 kg/s). Subsequently, the results obtained from this experiment were analysed using the analysis of variance (ANOVA) method. According to the data obtained from the ANOVA method and pairwise mean comparisons, the best configuration that yields the highest thermal performance was the one with counter flow passage (3 cm bed height, and 0.043 kg/s air flow rate). Moreover, a 99% confidence interval was utilized in estimating the lower and upper bounds of thermal performance for each system setup.

Key words: *Solar air heater, ANOVA, Thermal performance, Experimental design*

1. Introduction

The design and analysis of the experiment technique are applied in many fields in order to make discoveries about specific systems and/or processes [1]. Many statistical methodologies are used in the analysis of data in an experiment; one of such techniques is the analysis of variance (ANOVA). This technique has been utilized by many researchers in the analyses of various renewable energy sources such as solar energy systems [2]. Due to the rise in the amount of environmental pollutants and the rapid depletion of conventional energy sources, the necessity to utilize renewable energy sources has become crucial nowadays. Solar energy technologies are very common because these systems are available worldwide and produce less waste. Various studies have been conducted in order to improve the performance of such systems; one of them is a comprehensive study on various solar energy applications carried out by Sansaniwal et al. [3].

A typical flat-plate collector includes three important elements: an absorber plate, a transparent cover, and the collector housing. The main disadvantage of solar air collectors is the low efficiency that occurs due to the low heat transfer coefficient alongside the heat losses

that occur through the cover. In order to improve the thermal efficiency of solar collectors, researchers around the world have applied a number of various techniques.

Zhang et al. [4] examined the effects of significant factors on the thermal efficiency of a solar air heater with slit-perforated corrugated plates, both mathematically and experimentally. They found that among structure parameters, the absorber plate height had the strongest effect on the collector efficiency. Furthermore, it was discovered that at 1.14 m/s air velocity, the collector efficiency was approximately 67.83%, which is definitely better efficiency than the efficiencies of other transpired air collectors. Singh et al. [5] tested a solar collector with a V-down rib and indicated that the new system had better thermal efficiency compared to other similar collectors. In a similar study conducted by Rajaseenivasan et al. in 2015, two types of turbulators (V-type and circular) were connected to the absorber plate; thereafter, it was discovered that the obtained thermal efficiency was much higher when compared with the typical solar collectors [6]. An experimental study on a solar air heater with aluminium foil ducts was conducted in Turkey [7]. In that study, the system was tested with and without covers at three various mass flow rates (0.013 kg/s, 0.03 kg/s, and 0.044 kg/s), and the results were compared with those of a conventional solar air collector. In comparison with the flat collector, 5.9 - 41.2% higher efficiency was achieved from the newly designed collector. In another study, the shape of the absorber plate was modified in order to improve the area of heat transfer and the thermal performance of the collector. Protrusion plates, sinusoidal corrugated plates, and combined protrusion and sinusoidal corrugated shaped plates were manufactured and tested in an actual environment; thereafter, the results were compared with those of a collector that had a normal absorber sheet. The findings showed that using any of these absorber plates with new shapes in a flat plate solar collector increases the pressure drop, heat transfer coefficient, and performance factor in the system [8].

In an experimental study conducted by Komolafe et al. [9], rectangular rib roughness was used on the absorber part of the collector. The range of thermal efficiency calculated from the system was between 14 and 56.5%; additionally, the maximum values of ambient temperature, solar intensity, and solar air heater temperature were found to be 33.77 °C, 827.87 W/m^2, and 112 °C, respectively.

Seyedeh Sahar Hosseini et al. [10] examined numerically the effect of fin shadow on the mass flow rate, temperature, and performance of a solar air heater. Different fin shapes (elliptical, rectangular, and triangular) and various inclination angles (45-90°) were considered in their study. Their results showed that the fin shadow reduces the solar air heater performance by about 10 to 20%. In another study completed in India, the thermal performances of single- and double-pass solar air collectors with wavy wire mesh-packed beds were investigated both experimentally and numerically. Their experimental results showed that the thermohydraulic and thermal efficiencies of the double-pass solar air heater were about 74% and 80%, respectively. It was also discovered that the achieved efficiencies were 17% and 18% higher than the ones for single pass solar air heaters, respectively. In many studies, in order to increase the area of heat transfer, various objects like baffles [12]–[14], vortex generators [15] or fins [16]–[18] were attached to the absorber parts of collectors; however, it was found that these objects could increase the pressure drop within the solar collectors [19]. Many other studies present various methods for improving the factors affecting the performance of collectors [20]–[23].

This study aims to evaluate the performance of newly designed solar air heaters with different characteristics using the ANOVA method. There have been several innovations such

as the new solar air heater that was introduced with different characteristics; another novelty of the study is the estimation of the lower and upper bound of the system thermal performance under different configurations using a 99% confidence interval. Consequently, this paper is arranged in such a manner that the design procedure and the system setup are described first, and this is followed by an uncertainty analysis. Subsequently, analyses of the experiment using the ANOVA technique are presented and the results (that will reveal the best system setup necessary for the determination of thermal performance) are discussed in the last section.

2. Materials and Methods

2.1 Experimental procedure and system setup

The current solar air heaters have been designed and modified many times. A modified solar air heater was designed and manufactured to be tested experimentally in Istanbul, Turkey, during summertime. The process involved the testing of solar collectors as both single- and counter flow collectors using three different airflow rates; subsequently, the efficiency of each system was measured separately. One of the innovative contributions of this study is the creation of newly designed systems that are necessary to improve thermal performance.

Different system configurations were examined, and the data obtained from each setup was analysed using the analysis of variance (ANOVA) method. The novelty of this system was its simple design that facilitated the fabrication of the collector using cheap materials available in the local market. The pictorial representation and schematic diagrams of the tested solar air heater are shown in Figure 1.

The collector length, width, and height were 111.5 cm, 70.6 cm, and 13 cm, respectively. The whole frame was painted in matt black to improve absorptivity and reduce reflectivity from the walls. The collector bed height (the distance between the perforated glazing and the bottom of the collector) was changed from 3cm to 5cm and to 7 cm at each test set. The aim was to find the optimum bed height which would lead to high thermal performance; these characteristics are shown in Table 1. At each different bed height, the solar collector was examined as either a single or a counter flow system. To do so, the second glazing was placed on top of the first one to convert the system to a double-pass collector. In the case of a counter flow collector, the height of the second channel was 10 cm, 8 cm, and 6 cm at bed heights of 3 cm, 5 cm, and 7 cm, respectively. A vent with an area of 200 cm^2 was made in the mid part of the second cover to allow the air to enter the second channel of the collector and circulate in the system (Fig. 1). To reduce heat losses through the sides and bottom of the collector, the whole frame was covered with 3 cm thick Styrofoam boards. According to the geographical location of Istanbul, the collector tilt angle was fixed at 31º.

In this study, the absorber plate was replaced by metal wire meshes that acted as an absorber sheet; as a result, the construction cost of the solar air heater was reduced significantly as the wire mesh was much cheaper than the sheet metal plate that was readily available in the market. The absorptivity of wire meshes was increased as they were painted in black. The perforated cover was used instead of a normal one in order to reduce potential heat losses via the cover. Holes made in the first quarter on both the top and bottom parts of the cover would allow the air into the collector and cool it simultaneously. The perforated cover was made of Plexiglas; its length, width, and thickness were 106.5 cm, 66.5 cm, and 0.3 cm, respectively. While making holes of 0.3 cm in diameter, a distance of 3 cm was maintained between the centres of the holes.

Varieties of types of equipment were used alongside the main system to measure and record the data during the tests. An hourly solar radiation measurement was performed using an EKO-MS-410 F type Pyranometer, while the air temperature was measured by T-type thermocouples. Due to the need to read and record the air temperature at various locations and specific intervals, a few data loggers were utilized. TESTO 176 T4 type data loggers with a recording temperature range from -200 to 400 ºC and uncertainty of ±0.3 ºC were connected to several thermocouples that were placed at different positions on the collector. Inlet and outlet air temperatures in addition to the perforated cover surface temperature were all recorded hourly and the data from the loggers were transferred to the computer and evaluated with the help of Comfort software (version: 5.6 SP6.1.80.32798). Meanwhile, a centrifugal fan (Type: FBSY-1) in cooperation with an Allen-Bradley Power Flex 4M speed controller (Type: 22F-A8P0N103) was circulating the air through the collector.

The data recordings started at 9 a.m. and continued until 4 p.m. each day for different test sets. Each collector configuration was tested with three different air mass flow rates and the performance of each system was evaluated separately. The solar collector was tested as both a single and a counter flow collector, and the obtained results were analysed and compared.

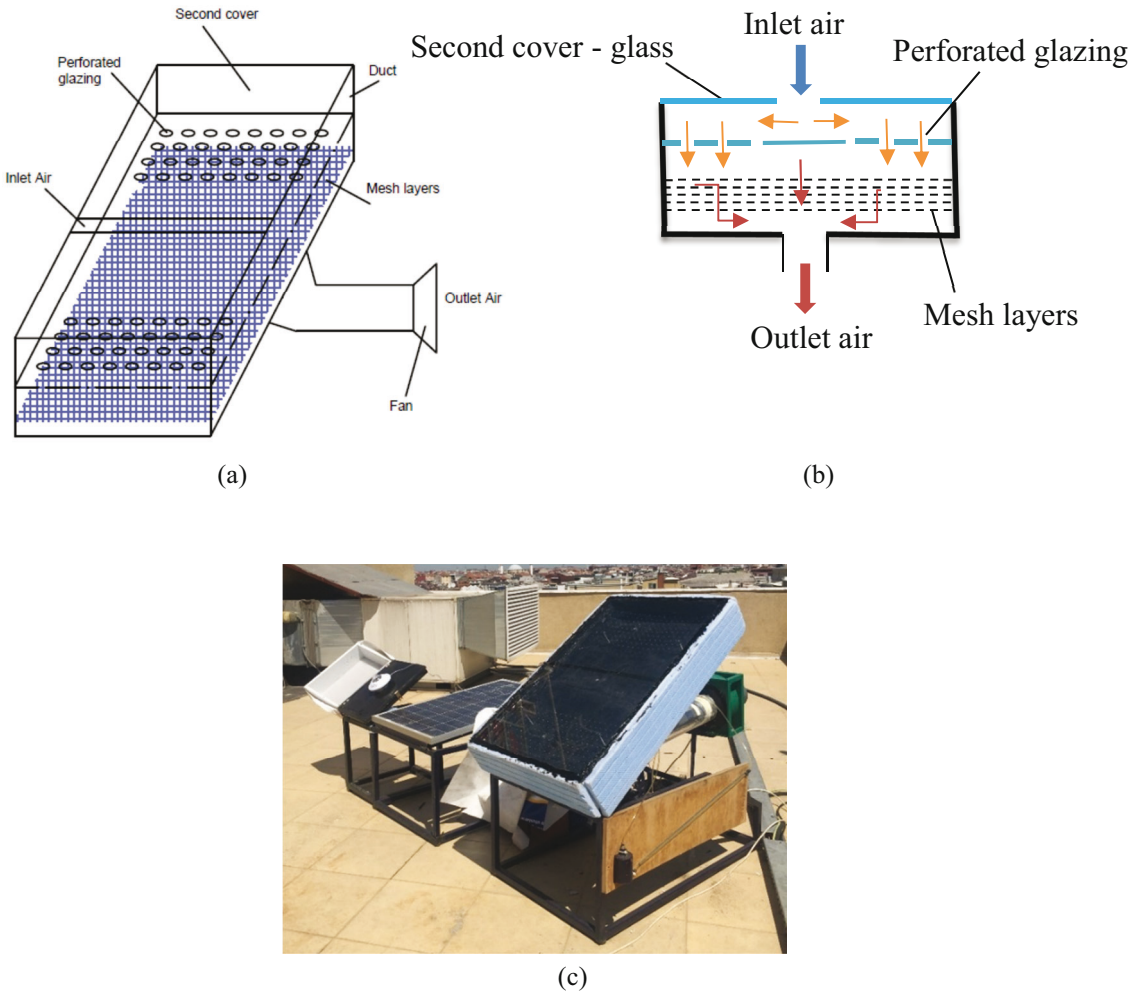

Fig. 1 a) A schematic diagram of the novel solar air collector, b) A side view of the collector, c) The pictorial representation of the system

Table 1 Characteristics of the solar air collector

Length /cm	111.5
Width /cm	70.6
Tilt angle /°	31
Bed height /cm	3, 5, 7
Inlet/outlet area /cm^2	200
Number of meshes	16
Glass cover: thickness, transmissivity	0.3 cm, $\tau = 0.86$
Pierced cover: thickness, hole diameter, distance btw. holes	0.3 cm, 0.3 cm, 3 cm
Insulation: material, thermal conductivity, thickness	Styrofoam, 0.033 W/m K, 3 cm

2.2 Model equations for performance evaluation

The thermal performance ($\boldsymbol{\eta_{th}}$) of the proposed solar air heater is calculated hourly for each different configuration of the system using equation 1:

$$\eta_{th} = \frac{\dot{m} * c_P * (T_{out} - T_{in})}{I * A_p} \tag{1}$$

where $\mathbf{C_p}$ is the air specific heat (J/kg K), ṁ is the air mass flow rate (kg/s), $\boldsymbol{T_{out}}$ and $\boldsymbol{T_{in}}$ are the outlet and inlet air temperatures (°C), respectively; $\boldsymbol{A_p}$ stands for the collector absorber area (m^2) and **I** is the solar intensity (W/m^2). To find the air mass flow rate through the collector, equation 2 is applied as follows:

$$\dot{m} = \rho_{air} * Q \tag{2}$$

where $\boldsymbol{\rho_{air}}$ is the air density at film temperature ( ) and $\boldsymbol{Q}$ is the volume flow rate of air. These are calculated using equations 3 and 4:

$$\Delta P = g * h * \left(\frac{A_2}{A_1} + 1\right) * (\rho_{Alcohol} - \rho_{air}) * \sin\theta \tag{3}$$

$$Q = CM * A_o * \sqrt{\frac{2}{\rho}} * \sqrt{\Delta P} \tag{4}$$

where $\boldsymbol{\Delta P}$ is the pressure drop (Pa), $\boldsymbol{g}$ is the gravitational acceleration (m/s^2), $\boldsymbol{A_1}$ and $\boldsymbol{A_2}$ are the monometer and its container areas (m^2), respectively; $\boldsymbol{\rho_{Alcohol}}$ is the alcohol density, $\boldsymbol{\theta}$ is the monometer tilt angle (degree), $\boldsymbol{CM}$ is the flow coefficient, and $\boldsymbol{A_o}$ is the orifice area (m^2).

2.3 System evaluation using the analysis of variance (ANOVA)

The design and analysis of this experiment technique have been widely used to examine the performance of various systems or processes (see Fig. 2) [1]. Using this method, it is possible to define an experiment as a series of tests in which purposeful changes to the input of a system or process will result in the output response [24]. The analysis of variance has different applications, but it has been used in few studies. For instance, Nowzari et al. employed ANOVA to develop a statistical model to find the best configuration (highest thermal efficiency) for a newly designed solar air heater [25]. The main objective of this type of study is to determine which factors (controllable or uncontrollable) have the greatest influence on the output.

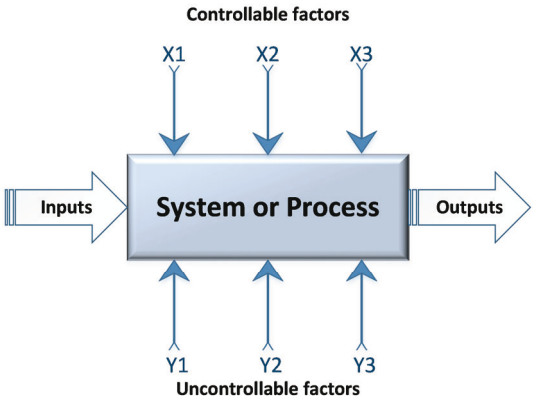

Fig. 2 A simple model of a system or process [1]

In this section, the general factorial design method was used in examining the experimental data. The results were poised on determining whether different factors have significant effects on the thermal performance of the system or not. The factors and their levels are as follows:

I. Bed height with three levels (3cm, 5cm, and 7 cm)
II. Collector type with two levels (single pass and counter flow)
III. Airflow rate with three levels (0.011kg/s, 0.035kg/s and 0.043kg/s)

The regression mathematical model for the performed experiment is written in equation 1; it presents a specific case for the three-factor factorial design.

$$P_{ijkl} = \mu + \tau_i + \beta_j + \gamma_k + (\tau\beta)_{ij} + (\tau\gamma)_{ik} + (\beta\gamma)_{jk} + (\tau\beta\gamma)_{ijk} + \varepsilon_{ijkl}$$

$$\begin{cases} i = 1,2,3 \\ j = 1,2 \\ k = 1,2,3 \\ l = 1,2,\dots,8 \end{cases} \quad (5)$$

In this model, $\boldsymbol{P_{ijkl}}$ represents the system thermal performance for the $\boldsymbol{l}$th observation when factor I (bed height) is at the $\boldsymbol{i}$th level, factor II (collector type) is at the $\boldsymbol{j}$th level, and factor III (air flow rate) is at the $\boldsymbol{k}$th level; $\boldsymbol{\mu}$ is the overall mean effect, $\boldsymbol{\tau_i}$ is the effect of the $\boldsymbol{i}$th level of factor I, $\boldsymbol{\beta_j}$ is the effect of the $\boldsymbol{j}$th level of factor II, $\boldsymbol{\gamma_k}$ is the effect of the $\boldsymbol{k}$th level of factor III, $\boldsymbol{(\tau\beta)_{ij}}$ is the effect of interaction between $\boldsymbol{\tau_i}$ and $\boldsymbol{\beta_j}$, $\boldsymbol{(\tau\gamma)_{ik}}$ is the effect of interaction between $\boldsymbol{\tau_i}$ and $\boldsymbol{\gamma_k}$, $\boldsymbol{(\beta\gamma)_{jk}}$ is the effect of interaction between $\boldsymbol{\beta_j}$ and $\boldsymbol{\gamma_k}$, $\boldsymbol{(\tau\beta\gamma)_{ijk}}$ is the effect of interaction between $\boldsymbol{\tau_i}$, $\boldsymbol{\beta_j}$ and $\boldsymbol{\gamma_k}$, and $\boldsymbol{\varepsilon_{ijkl}}$ is the random error component. For each combination, 8 observations are recorded from 9 a.m. to 4 p.m. The testing hypotheses about the equality effects of levels of factors I, II, and III are given respectively as follows:

$$H_0: \beta_1 = \beta_2 = \beta_3 = 0 \quad (6)$$
$$H_1: \text{at least one } \beta_j \neq 0$$

$$H_0: \tau_1 = \tau_2 = 0 \quad (7)$$
$$H_1: \text{at least one } \tau_i \neq 0$$

$$H_0: \gamma_1 = \gamma_2 = \gamma_2 = 0 \quad (8)$$
$$H_1: \text{at least one } \gamma_k \neq 0$$

Similarly, to determine whether the levels of factors I, II, and III interact, equations (6) to (8) are developed. The interaction between the levels of factors I, II, and III are:

$$H_0: (\tau\beta)_{ij} = 0 \text{ for all } i,j \quad (9)$$
$$H_1: \text{at least one } (\tau\beta)_{ij} \neq 0$$

$$H_0: (\tau\gamma)_{ik} = 0 \text{ for all } i,k \quad (10)$$
$$H_1: \text{at least one } (\tau\gamma)_{ik} \neq 0$$

$$H_0: (\beta\gamma)_{jk} = 0 \text{ for all } j,k \quad (11)$$
$$H_1: \text{at least one } (\beta\gamma)_{jk} \neq 0$$

$$H_0: (\tau\beta\gamma)_{ijk} = 0 \text{ for all } i,j,and\ k \quad (12)$$
$$H_1: \text{at least one } (\tau\beta\gamma)_{ijk} \neq 0$$

The model and hypotheses were considered and tested for thermal performance; thereafter, the results of the analysis of variance (ANOVA) were computed and are presented in the following section. The significant level of the test (α) is considered as 0.01. It is imperative to note that the IBM SPSS 16 statistical package was used for computational analysis.

3. Results and Discussion

Based on the results shown in Table 2, the following conclusions can be drawn for each factor:

• H_0 in equations (6), (7), and (8) were rejected, so it is possible to conclude that all factors (I, II, III) have a significant effect on the thermal performance of the system. In other words, there are significant differences between the mean levels of each factor, and it means that there is a substantial change in thermal performance when the factor levels are changed. At this point it possible to start comparing the levels of each factor (I, II, and III) to find out which level of each factor led to the highest thermal performance in the system.

• We failed to reject H_0 in equations (9)-(12). Therefore, it is possible to say that there were no interactions between all factors. In other words, when all three factors are considered for analysis, their levels do not interact with each other.

Table 2 Analysis of variance results for mean total throughput time

Source of variation	Sum of Squares	Degree of Freedom	Mean Square	F_0	*P*-Value
Corrected Model	11096.48	17	652.73	3.819	
Intercept	267519.11	1	267519.11	1565.179	
Bed height (BH)	4794.6	2	2397.31	14.026	0.000*
Collector type (CT)	1984.62	1	1984.62	11.611	0.001*
Air flow rate (AFR)	4158.3	2	2079.18	12.165	0.000*
BH × CT	16.63	2	8.31	0.049	0.953
BH × AFR	80.62	4	20.15	0.118	0.976
CT × AFR	49.33	2	24.66	0.144	0.866
BH × CT × AFR	12.28	4	3.07	0.018	0.999
Error	21535.82	126	170.91		
Total	300151.4	144			
Corrected Total	32632.309	143			

* Indicates that the factor has a significant effect on the system thermal performance

It is concluded that there are significant differences between the mean levels of bed heights (Table 2). As it is shown in Fig. 3, the solar collector with a bed height of 3cm yields the highest estimated marginal mean of thermal performance when compared to the others. To validate this conclusion, three different methods were used to test all pairwise mean comparisons. Tukey's Honestly Significant Difference (HSD) method, Fisher's Least Significant Difference (LSD) method, and Dunnett's method are the three tests that were used for comparison. The obtained results are shown in Table 3 at $\alpha = 0.01$ level.

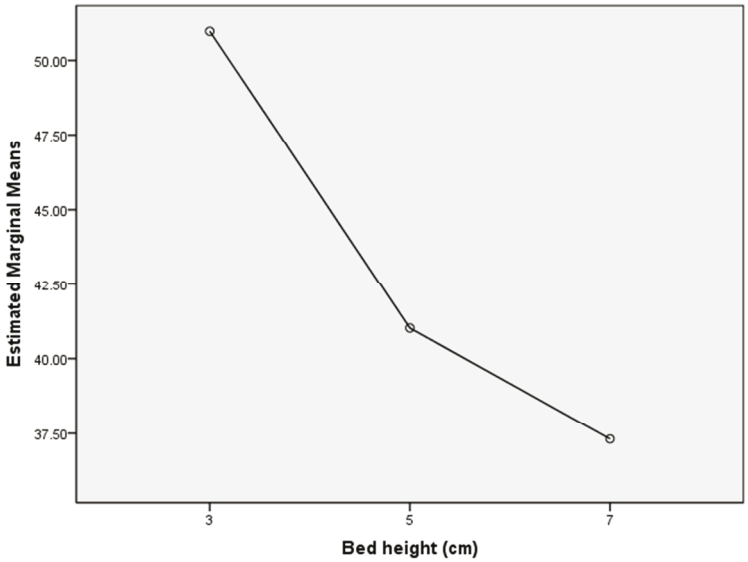

Fig. 3 Estimated marginal mean of thermal performance for different bed heights

Table 3 Pairwise mean comparisons for different bed heights

Method	(I) Bed height /cm	(J) Bed height /cm	Mean Difference (I-J)
Tukey's HSD	3	5	9.9579*
		7	13.6658*
	5	3	-9.9579*
		7	3.7079
	7	3	-13.6658*
		5	-3.7079
LSD	3	5	9.9579*
		7	13.6658*
	5	3	-9.9579*
		7	3.7079
	7	3	-13.6658*
		5	-3.7079
Dunnett	3	7	13.6658*
	5	7	3.7079

* Indicates significant differences between mean levels at $\alpha = 0.01$

In the case of the collector type, the preferred level is counter flow. When assessing the changes in thermal performance in Fig. 4, the counter flow collectors result in higher values of estimated marginal mean when compared with the single pass collectors.

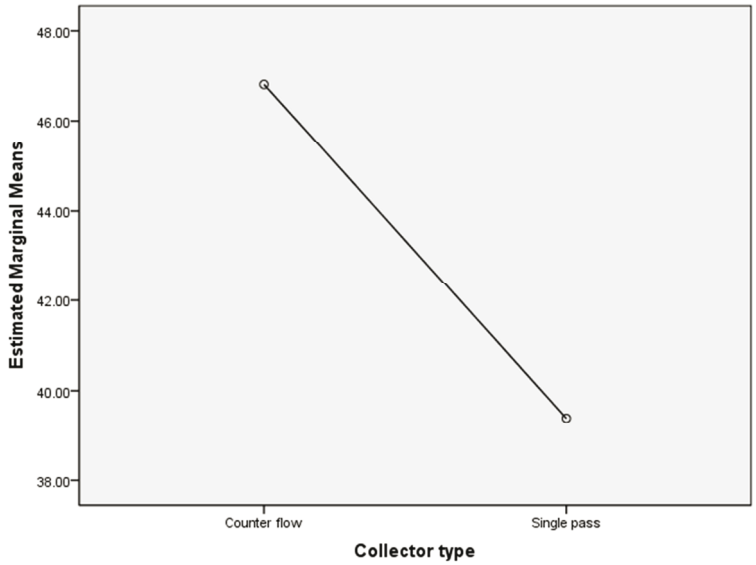

Fig. 4 Estimated marginal mean of thermal performance for different collector types

The airflow rate is another important factor that affects the system thermal performance. In Fig. 5 one can clearly see that when the airflow rate is increased, the estimated marginal mean is increased as well. Consequently, it is possible to conclude that the optimal airflow is 0.043 kg/s. To prove this conclusion, Tukey's HSD, Fisher's LSD, and Dunnett's methods were applied for comparison; the results are given in Table 4.

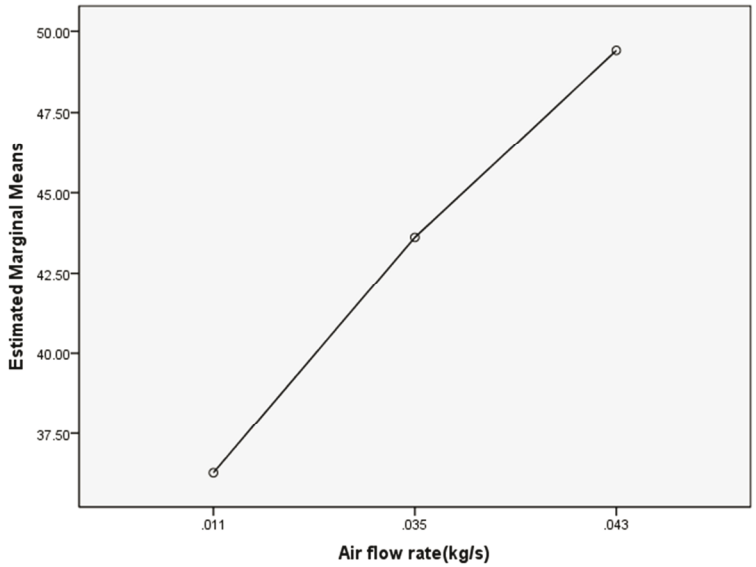

Fig .5 Estimated marginal mean of thermal performance for different collector types

Table 4 Pairwise mean comparisons for different air flow rates

Method	(I) Air flow rate / kg/s	(J) Air flow rate / kg/s	Mean Difference (I-J)
Tukey's HSD	0.011	0.035	-7.3371
		0.043	-13.1329*
	0.035	0.011	7.3371
		0.043	-5.7958
	0.043	0.011	13.1329*
		0.035	5.7958

Method	(I) Air flow rate / kg/s	(J) Air flow rate / kg/s	Mean Difference (I-J)
LSD	0.011	0.035	-7.3371*
		0.043	-13.1329*
	0.035	0.011	7.3371*
		0.043	-5.7958
	0.043	0.011	13.1329*
		0.035	5.7958
Dunnett	0.011	0.043	-13.1329*
	0.035	0.043	-5.7958

* Indicates significant differences between mean levels at $\alpha = 0.01$

When all three factors are considered (see Fig. 6), it can be seen that the maximum estimated marginal mean of the system thermal performance is achieved when factor I (bed height) is at level 1 (3 cm), factor II (collector type) at level 2 (counter flow), and factor III (air flow rate) at level 3 (0.043 kg/s). In this case, the estimated marginal mean of the system thermal performance is 60.78%.

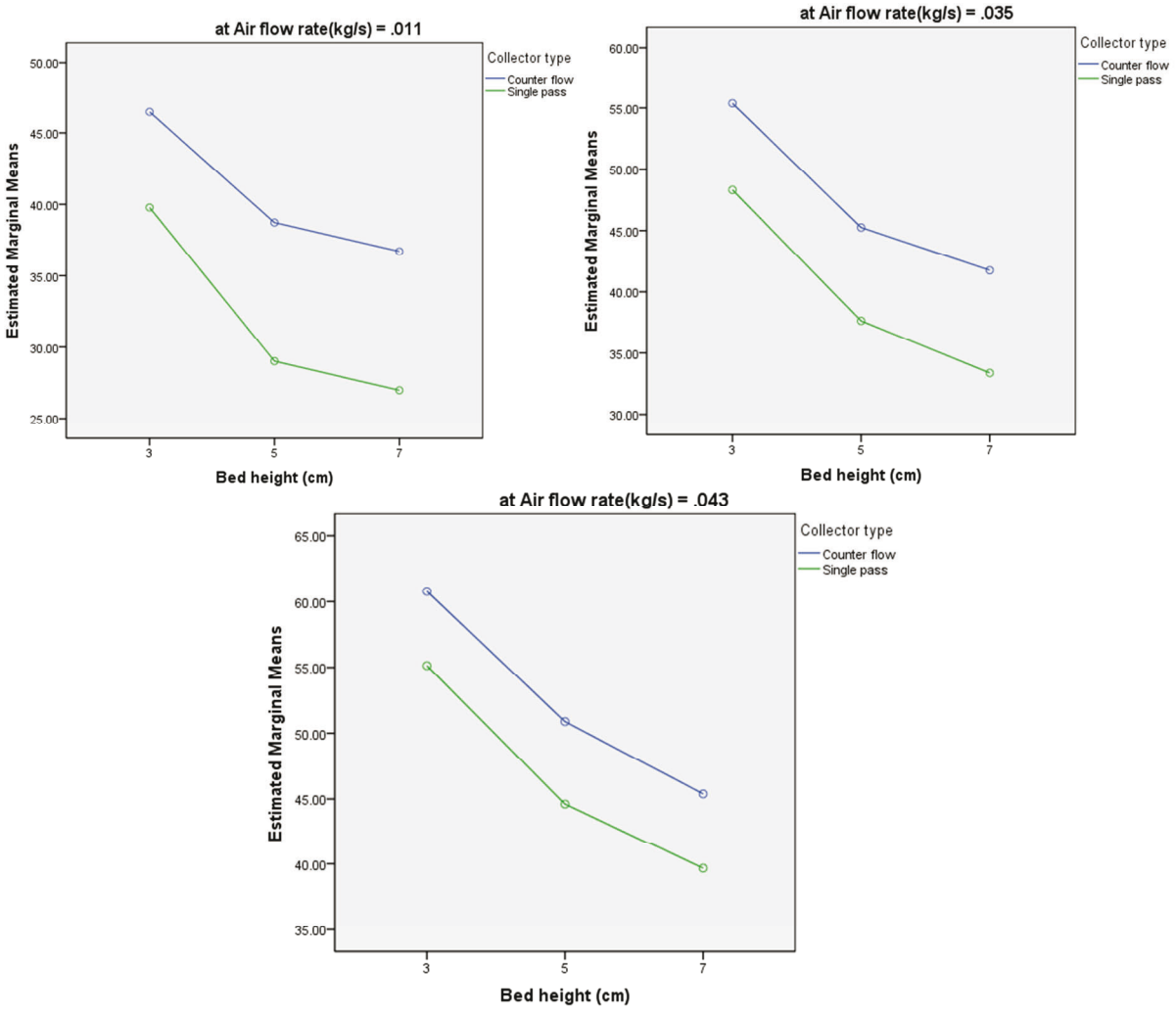

Fig.6 Estimated marginal mean of thermal performance (%) with respect to bed height, collector types and airflow rate.

Moreover, it is possible to estimate the system thermal performance for different configurations. In Table 5, the thermal performance is estimated with 99% confidence interval to discover the response of the system under different configurations for factors and their levels. In this table, the lower/minimum-bound and upper/maximum-bound estimated thermal performances for the system are computed. For instance, the lowest estimated thermal performance (14.890%) would be obtained when the bed height is 7 cm, the collector type is a single pass, and the airflow rate is 0.011 kg/s. Similarly, the highest estimated thermal performance (72.872%) would be obtained when the bed height is 3 cm, the collector type is counter flow, and airflow rate is 0.043 kg/s.

Table 5 Estimated system thermal performance with 99% confidence interval

Bed height /cm	Collector type	Airflow rate / kg/s	99% Confidence Interval	
			Lower Bound	Upper Bound
3	Counter flow	**0.011**	34.380	58.558
		0.035	43.286	67.464
		0.043	48.693	72.872**
	Single pass	**0.011**	27.690	51.868
		0.035	36.225	60.403
		0.043	43.051	67.229
5	Counter flow	**0.011**	26.635	50.813
		0.035	33.161	57.339
		0.043	38.795	62.973
	Single pass	**0.011**	16.923	41.102
		0.035	25.541	49.719
		0.043	32.522	56.700
7	Counter flow	**0.011**	24.620	48.798
		0.035	29.661	53.839
		0.043	33.297	57.475
	Single pass	**0.011**	14.890*	39.068
		0.035	21.286	45.464
		0.043	27.576	51.754

* Indicates the lowest thermal performance; ** Indicates the highest thermal performance.

4. Conclusion

The use of renewable energy is growing every day due to the reduction in fossil fuel resources and climate changes. In this study, the design and analysis of the experimental method were used to analyse different configurations of a newly designed solar air heater with respect to their thermal performances. Metal mesh layers are used to improve the heat transfer between the airstream and the absorber. Three main parameters were changed in the system to see the effect on thermal performance. Those parameters were bed height (3 cm, 5 cm, and 7 cm), collector type (single pass and counter flow), and airflow rate (0.011 kg/s, 0.035 kg/s, and 0.043 kg/s). The experiments were performed in an actual environment.

Based on the results obtained via the ANOVA analysis, it is concluded that the collector type, bed height, and airflow rate have significant effects on the thermal performance of a collector. Additionally, pairwise mean comparisons were applied to find the best system setup

that would yield the highest thermal performance. The results obtained showed that the highest thermal performance was achieved from the collector with a counter flow passage, bed height of 3 cm, and air flow rate of 0.043 kg/s. Finally, the upper and lower bounds for the thermal performance of the system were estimated with a 99% confidence interval. The estimated model helped to approximate the highest and the lowest system performance under different configurations. Therefore, this model can be used to estimate the thermal efficiency of a collector with different configurations. The lowest estimated thermal performance (14.890%) belongs to the system configuration when the bed height is 7 cm, the collector type is a single pass, and the airflow rate is 0.011 kg/s. On the other hand, the highest estimated thermal performance (72.872%) can be achieved when the bed height is 3 cm, the collector type is counter flow, and the airflow rate is 0.043 kg/s.

In future studies, mathematical models developed by simulation modelling and analysis using current data to estimate the system performance for newly designed systems might definitely evolve as there are plans to ensure that this happens.

REFERENCES

[1] D. C. Montgomery, Design and Analysis of Experiments, 10th Edition, 10th ed. WILEY, 2019.

[2] H. Saygin, R. Nowzari, N. Mirzaei, and L. B. Y. Aldabbagh, "Performance evaluation of a modified PV/T solar collector: A case study in design and analysis of experiment," Sol. Energy, vol. 141, 2017. https://doi.org/10.1016/j.solener.2016.11.048

[3] S. K. Sansaniwal, V. Sharma, and J. Mathur, "Energy and exergy analyses of various typical solar energy applications: A comprehensive review," Renew. Sustain. Energy Rev., vol. 82, pp. 1576-1601, Feb. 2018. https://doi.org/10.1016/j.rser.2017.07.003

[4] H. Zhang et al., "Mathematical modeling and performance analysis of a solar air collector with slit-perforated corrugated plate," Sol. Energy, vol. 167, pp. 147-157, Jun. 2018. https://doi.org/10.1016/j.solener.2018.04.003

[5] S. Singh, S. Chander, and J. S. Saini, "Thermo-hydraulic performance due to relative roughness pitch in V-down rib with gap in solar air heater duct-Comparison with similar rib roughness geometries," Renew. Sustain. Energy Rev., vol. 43, pp. 1159-1166, Mar. 2015. https://doi.org/10.1016/j.rser.2014.11.087

[6] T. Rajaseenivasan, S. Srinivasan, and K. Srithar, "Comprehensive study on solar air heater with circular and V-type turbulators attached on absorber plate," Energy, vol. 88, pp. 863-873, Aug. 2015. https://doi.org/10.1016/j.energy.2015.07.020

[7] S. Şevik and M. Abuşka, "Thermal performance of flexible air duct using a new absorber construction in a solar air collector," Appl. Therm. Eng., vol. 146, pp. 123-134, Jan. 2019. https://doi.org/10.1016/j.applthermaleng.2018.09.100

[8] S. Li, H. Wang, X. Meng, and X. Wei, "Comparative study on the performance of a new solar air collector with different surface shapes," Appl. Therm. Eng., vol. 114, pp. 639-644, Mar. 2017. https://doi.org/10.1016/j.applthermaleng.2016.12.026

[9] C. A. Komolafe, I. O. Oluwaleye, O. Awogbemi, and C. O. Osueke, "Experimental investigation and thermal analysis of solar air heater having rectangular rib roughness on the absorber plate," Case Stud. Therm. Eng., vol. 14, p. 100442, Sep. 2019. https://doi.org/10.1016/j.csite.2019.100442

[10] S. S. Hosseini, A. Ramiar, and A. A. Ranjbar, "The effect of fins shadow on natural convection solar air heater," Int. J. Therm. Sci., vol. 142, pp. 280-294, Aug. 2019. https://doi.org/10.1016/j.ijthermalsci.2019.04.015

[11] S. Singh, "Experimental and numerical investigations of a single and double pass porous serpentine wavy wiremesh packed bed solar air heater," Renew. Energy, vol. 145, pp. 1361-1387, Jan. 2020. https://doi.org/10.1016/j.renene.2019.06.137

[12] K. Mohammadi and M. Sabzpooshani, "Comprehensive performance evaluation and parametric studies of single pass solar air heater with fins and baffles attached over the absorber plate," Energy, vol. 57, pp. 741-750, Aug. 2013. https://doi.org/10.1016/j.energy.2013.05.016

[13] K. Mohammadi and M. Sabzpooshani, "Appraising the performance of a baffled solar air heater with external recycle," Energy Convers. Manag., vol. 88, pp. 239-250, Dec. 2014. https://doi.org/10.1016/j.enconman.2014.08.009

[14] H.-M. Yeh, C.-D. Ho, and C.-Y. Lin, "Effect of collector aspect ratio on the collector efficiency of upward type baffled solar air heaters," Energy Convers. Manag., vol. 41, no. 9, pp. 971-981, Jun. 2000. https://doi.org/10.1016/S0196-8904(99)00148-X

[15] S. Tamna, S. Skullong, C. Thianpong, and P. Promvonge, "Heat transfer behaviors in a solar air heater channel with multiple V-baffle vortex generators," Sol. Energy, vol. 110, pp. 720-735, Dec. 2014. https://doi.org/10.1016/j.solener.2014.10.020

[16] S. Singh, L. Dhruw, and S. Chander, "Experimental investigation of a double pass converging finned wire mesh packed bed solar air heater," J. Energy Storage, vol. 21, pp. 713-723, Feb. 2019. https://doi.org/10.1016/j.est.2019.01.003

[17] R. Kumar and M. A. Rosen, "Performance evaluation of a double pass PV/T solar air heater with and without fins," Appl. Therm. Eng., vol. 31, no. 8-9, pp. 1402-1410, Jun. 2011. https://doi.org/10.1016/j.applthermaleng.2010.12.037

[18] A. A. El-Sebaii, S. Aboul-Enein, M. R. I. Ramadan, S. M. Shalaby, and B. M. Moharram, "Thermal performance investigation of double pass-finned plate solar air heater," Appl. Energy, vol. 88, no. 5, pp. 1727-1739, May 2011. https://doi.org/10.1016/j.apenergy.2010.11.017

[19] L. Abhay, V. P. Chandramohan, and V. R. K. Raju, "Numerical analysis on solar air collector provided with artificial square shaped roughness for indirect type solar dryer," J. Clean. Prod., vol. 190, pp. 353-367, Jul. 2018. https://doi.org/10.1016/j.jclepro.2018.04.130

[20] M. Yu et al., "Experimental Investigation of a Novel Solar Micro-Channel Loop-Heat-Pipe Photovoltaic/Thermal (MC-LHP-PV/T) System for Heat and Power Generation," Appl. Energy, vol. 256, p. 113929, Dec. 2019. https://doi.org/10.1016/j.apenergy.2019.113929

[21] B. E. Moon and H. T. Kim, "Evaluation of thermal performance through development of a PCM-based thermal storage control system integrated unglazed transpired collector in experimental pig barn," Sol. Energy, vol. 194, pp. 856-870, Dec. 2019. https://doi.org/10.1016/j.solener.2019.11.009

[22] F. Calise, M. D. D'Accadia, and M. Vicidomini, "Optimization and dynamic analysis of a novel polygeneration system producing heat, cool and fresh water," Renew. Energy, vol. 143, pp. 1331-1347, Dec. 2019. https://doi.org/10.1016/j.renene.2019.05.051

[23] C. Qin, J. B. Kim, and B. J. Lee, "Performance analysis of a direct-absorption parabolic-trough solar collector using plasmonic nanofluids," Renew. Energy, vol. 143, pp. 24-33, Dec. 2019. https://doi.org/10.1016/j.renene.2019.04.146

[24] V. L. Anderson and R. A. McLean, Design of experiments : a realistic approach, 1st ed. New York : Marcel Dekker, 1974.

[25] R. Nowzari, N. Mirzaei, and L. B. Y. Aldabbagh, "Finding the best configuration for a solar air heater by design and analysis of experiment," Energy Convers. Manag., vol. 100, 2015. https://doi.org/10.1016/j.enconman.2015.04.058

Submitted: 11.4.2021

Accepted: 13.9.2021

Nima Mirzaei
Industrial Engineering Department,
Istanbul Aydin University, 34295 Sefakoy,
Istanbul, Turkey
nimamirzaei@aydin.edu.tr